IEEE Access
Multidisciplinary | Rapid Review | Open Access Journal

Received 1 December 2022, accepted 25 January 2023, date of publication 2 February 2023, date of current version 8 February 2023.

Digital Object Identifier 10.1109/ACCESS.2023.3241854

RESEARCH ARTICLE

Metaheuristic Optimization Techniques Used in Controlling of an Active Magnetic Bearing System for High-Speed Machining Application

SURAJ GUPTA[1], (Graduate Student Member, IEEE), PABITRA KUMAR BISWAS[1], (Member, IEEE), SUKANTA DEBNATH[1], ANUMOY GHOSH[2], THANIKANTI SUDHAKAR BABU[3], (Senior Member, IEEE), HOSSAM M. ZAWBAA[4,5,6], AND SALAH KAMEL[7]

[1]Department of Electrical and Electronics Engineering, National Institute of Technology Mizoram, Aizawl 796012, India
[2]Department of Electronics and Communication Engineering, National Institute of Technology Mizoram, Aizawl 796012, India
[3]Department of Electrical and Electronics Engineering, Chaitanya Bharathi Institute of Technology, Hyderabad 500075, India
[4]Faculty of Computers and Artificial Intelligence, Beni-Suef University, Beni Suef 62511, Egypt
[5]CeADAR Irelands Center for Applied AI, Technological University Dublin, Dublin, D07 EWV4 Ireland
[6]Applied Science Research Center, Applied Science Private University, Amman 11931, Jordan
[7]Department of Electrical Engineering, Faculty of Engineering, Aswan University, Aswan 81542, Egypt

Corresponding author: Hossam M. Zawbaa (hossam.zawbaa@gmail.com)

The work of Hossam M. Zawbaa was supported by the European Union's Horizon 2020 Research and Enterprise Ireland under the Marie Skłodowska-Curie Grant 847402.

ABSTRACT Smart control tactics, wider stability region, rapid reaction time, and high-speed performance are essential requirements for any controller to provide a smooth, vibrationless, and efficient performance of an in-house fabricated active magnetic bearing (AMB) system. In this manuscript, three pre-eminent population-based metaheuristic optimization techniques: Genetic algorithm (GA), Particle swarm optimization (PSO), and Cuckoo search algorithm (CSA) are implemented one by one, to calculate optimized gain parameters of PID controller for the proposed closed-loop active magnetic bearing (AMB) system. Performance indices or, objective functions on which these optimization techniques are executed are integral absolute error (IAE), integral square error (ISE), integral time multiplied absolute error (ITAE), and integral time multiplied square error (ITSE). The significance of an optimization technique and objective function can obtain only by implementing it. As a result, several comparisons are made based on statistical performance, time domain, frequency response behavior, and algorithm execution time. Finally, the applicability of optimization strategies in addition to the performance indices is determined with the aid of the comparative analysis. That could assist in choosing a suitable optimization technique along with a performance index for a high-speed application of an active magnetic bearing system.

INDEX TERMS Active magnetic bearing, genetic algorithm, cuckoo search algorithm, particle swarm optimization.

I. INTRODUCTION

In this century, high speed becomes a trend and an essential requirement in many research areas, like transportation, machine tools, manufacturing processes, semiconductor equipment, etc. It is well-known that active magnetic bearings (AMBs) are an inevitable alternative to conventional bearings in high-speed applications [1]. AMB belongs to the family of magnetic bearings which are capable of reaching very high speeds. The function of magnetic bearings rely on the phenomena of magnetic levitation [2], the hovering of a ferromagnetic object (rotor) with the help of a magnetic field. If the generation of the magnetic field is with the help of electromagnets then this

The associate editor coordinating the review of this manuscript and approving it for publication was Kuo-Ching Ying.

magnetic bearing is categorized as an active magnetic bearing [3].

For decades, active magnetic bearing (AMB) has attracted a lot of researchers' interest. Due to its non-contact characteristic compared to traditional bearings, it has a wide range of applications in the industry [4]. This non-contact feature of AMB is the cause of the near-zero friction (almost zero friction) between the stationary stator and rotating rotor, which eliminates the need for lubricants. The almost zero friction empowers the AMB system to attend the maximum allowable speed with less or, no vibrations, resulting in increased efficiency. The absence of lubricants minimizes the risk of oil contamination and increases the maintenance intervals.

Active magnetic bearings are being used in a wide range of applications such as Biomedical industries [5], [6], high-speed machining [7], [8], renewable energy [9], [10], aerospace [11] etc. Apart from the advantages, AMB has some limitations and challenges. The presence of electromagnetic forces and fields in AMB causes the formation of nonlinear Lorentz forces and electromagnetic inferences. This makes the AMB system inherently nonlinear. Other than these nonlinearities, the AMB system suffers from some system-based dynamic uncertainties [12]. To deal with the uncertainties and nonlinearities of AMB, in various research articles authors have taken the help of some intelligent optimization algorithms for controlling purposes. Chen and Chang optimized a PID controller for an active magnetic bearing system using a genetic algorithm [13]. Yanhong et al. implemented the particle swarm optimization (PSO) algorithm to optimize the PID controller for a magnetic levitation system [14], and Štimac et al. tuned the PID controller using the PSO algorithm. Dhyani et al. optimized a fuzzy-PID controller using Moth -flame optimization and compare it performance with a PID controller for active magnetic bearing system [15].

Optimization methods will be used to further improve the performance of the PID controller [16], [17]. Several prestigious researchers from around the world have contributed to this field. Like, Jain et al. implemented grey wolf optimization (GWO)/proportional-integral-derivative (PID) with IAE, ISE, ITAE, and ITSE objective functions and compared the performance among them [18]. Izci et al. optimized a PID controller using the slime mould algorithm (SMA) and compared it performance with other famous metaheuristic algorithms [19]. Ekinci et al. proposes a novel optimization approach which is Henry gas solubility optimization with opposition-based learning (OBL/HGO). This optimization technique is used to find out the best parameters of the PID controller using the integral of time multiplied absolute error (ITAE) objective function [20]. Guo Lei et al. proposes an improved mayfly algorithm based on the median position of the group. This algorithm reduced the optimal ITAE index value of the system when used to optimize a PID parameters [21]. Izci et al. developed a novel hybrid technique, arithmetic optimization algorithm- Nelder-Mead (AOA-NM) to achieve an optimum design for automobile cruise control [22]. Peicheng et al. combined the improved model predictive control (MPC) with a hybrid PID control to enhance the accuracy of path tracking in intelligent vehicles [23]. Later, Ekinci et al. proposes a novel metaheuristic optimization algorithm, logarithmic spiral-arithmetic optimization algorithm (Ls-AOA) [24] and further developed Lévy flight-based reptile search algorithm to improve the performance of PID controller [25].

Generally, the metaheuristic optimization methods are classified as, single solution based and population-based metaheuristic optimization techniques [26]. Single-solution based metaheuristics are pattern search, simulated annealing, tabu search etc. and population-based optimization techniques are GA, artificial bee colony, PSO etc. There is not any accessible way via a best optimization method may be picked among the numerous available optimization approaches. The only way to know the efficacy of any optimization approach is by applying it in any problem. The relevance of the particular optimization approach is demonstrated by the obtained outcomes of that problem. In certain cases, the same optimization approach may perform differently in multiple applications. In this study, the impact of three distinct optimization approaches on the proposed system will be examined. The very first will be the most famous evolutionary-based optimization algorithm i.e., the Genetic algorithm, which can apply to almost all complex problems and systems. The second is a swarm-based optimization algorithm, i.e., PSO. The absence of a genetic operator in PSO makes it much more flexible and versatile. And the third optimization method is CSA which is based on the brood breeding strategy of several species of cuckoo birds. As compared to other optimization method CSA have fewer tuning parameter which makes it simpler to use and faster in execution. A comparison of their results will demonstrate the effectiveness of each optimization approach.

The novelty of the manuscript is represented as depicted in Figure 1 and as follows-

1. In-house prototype of an active magnetic bearing system is fabricated. The electromagnet and rotor are made of ferromagnetic material having a higher value of relative permeability (5000 for the electromagnet and 11000 for the rotor). The copper coils (having relative permeability $\approx$ 1) are wounded on the electromagnet.

2. Nonlinearities and dynamic uncertainties of AMB systems make them complex to analyze and design. Therefore, using the physical parameters of the proposed AMB system a transfer function is calculated at a nominal point of operation (i_o, x_o).

3. For better controlling and bearing action, the Genetic algorithm, particle swarm optimization algorithm, and cuckoo search algorithm are used to calculate the gain values of the PID controller. Which is in the proposed closed loop.

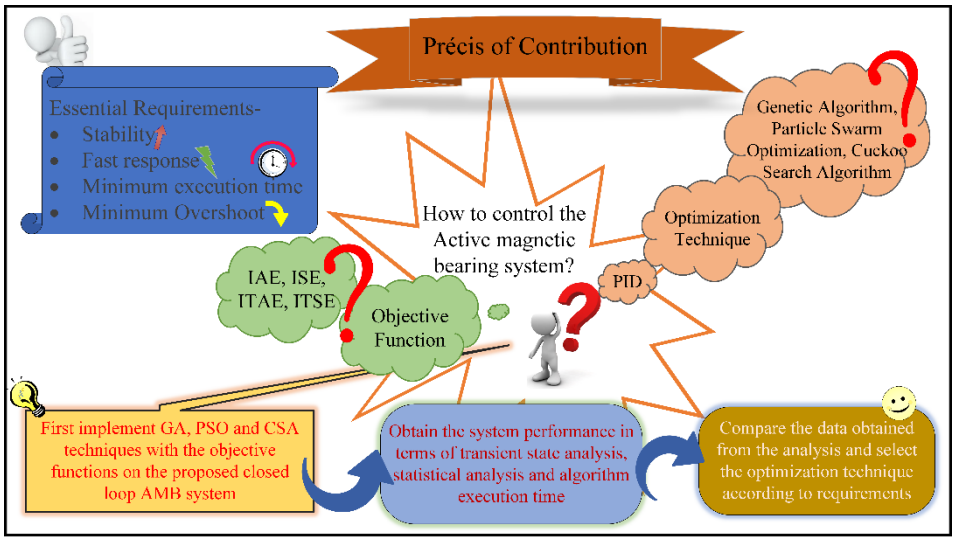

FIGURE 1. Core contribution of the manuscript.

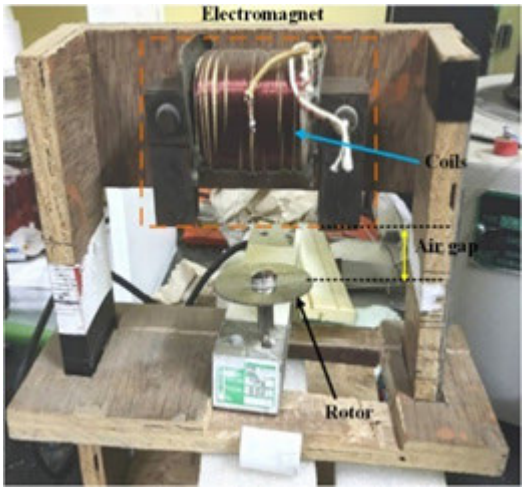

FIGURE 2. In-house prototype of proposed active magnetic bearing (AMB) system.

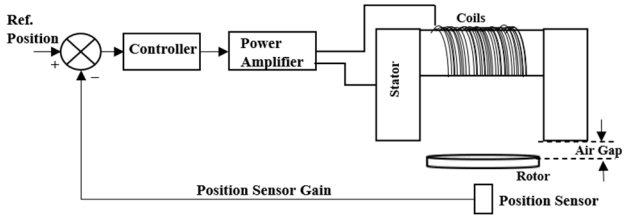

FIGURE 3. Simplified diagram of the active magnetic bearing system.

4. Each metaheuristic optimization algorithm is calibrated on the scale of four performance indexes (IAE, ISE, ITAE, and ITSE).

5. A fair comparison is carried out among these algorithms on the basis of their transient state performance incorporated with a bode plot, root locus plot, and Nyquist plot analysis. Further, parameters for compassion are statistical analysis and fastness in the execution of the algorithm.

The organization of the manuscript is arranged as follows:

Section II deals with the study of the constructional and linearized model of the proposed active magnetic bearing (AMB) system. Section III comprises of Application of optimization techniques for AMB system along with necessary flow charts. Section IV deals with the results and discussion which comprises of implementation of considered algorithms for proposed AMB system. Section V comprises of performance study and analysis of prosed system, finally section VI concludes the complete carried-out out work and future description of the work for future researchers.

The flowcharts for the three optimization strategies that were chosen are briefly described in Section III. The performance evaluation of various optimization approaches with various objective functions is the main emphasis of Section IV, followed by concluding observations.

II. PROPOSED IN-HOUSE MODEL OF AMB SYSTEM

In house model of the proposed active magnetic bearing (AMB) system is shown in Figure 2. The electromagnet and rotor are made of ferromagnetic material having a higher value of relative permeability (5000 for the electromagnet and 11000 for the rotor) [27]. The copper coils (having relative permeability ≈ 1) are wounded on an electromagnet having N numbers of turns.

In Figure 3, the position sensor detects the rotor's current location and creates a signal equivalent to the position. The difference between the reference signal (a unit step signal) and the position sensor's signal is an error signal. This error signal shows the deviation of the rotor from its actual or nominal position. To get the rotor to align in the nominal position a controller is implemented to produce a controlling signal which is further fed to the power amplifier [28], [29]. The power amplifier generates the required current and energies the coils of the electromagnet to create a sufficient magnetic

TABLE 1. In-house model parameter of the proposed AMB system.

Sl. No.	Parameter	Values	Unit
1.	Mass of rotor (m)	0.0654	Kg
2.	Coil Resistance (R)	1.2	Ω
3.	Coil inductance (L) at x_o airgap	0.020598	H
4.	K_a	0.5	N/A
5.	K_z	122.108	N/m
At nominal point,			
1.	i_o	2.44	A
2.	x_o	0.01	m

force for maintaining the rotor position at the nominal point of operation, against gravity.

Nonlinearities and dynamic uncertainties of AMB systems make them complex to analyze and design. Therefore, for a nominal point (i_o, x_o) of operation, the proposed system is linearized [30], [31] and can be written in a transfer function form as depicted in Equation 1, [32],

$$\frac{\Delta X(s)}{\Delta I(s)} = -\frac{K_a}{ms^2 - K_z} \tag{1}$$

where, K_a and K_z are force constants whose values depend on the physical parameters of the AMB system that is shown in Table 1. $\Delta X(s)$ is s-domain transformation of a small change $\Delta x\,(t)$ in the position of the rotor and due to this the change in the coil current $\Delta i\,(t)$ in s-domain is $\Delta I(s)$.

For a nominal point of operation, the proposed AMB system is calculated in a form of a transfer function using the data available in Table 1. i.e.,

$$C_{AMB} = \frac{\Delta X(s)}{\Delta I(s)} = \frac{7.69}{s^2 - 1877.49} \tag{2}$$

In this study, all of the optimizations are performed for the nominal point (Equation 2) of operation. This will help in making a clear and fair comparison among the performances of optimization techniques. The next section will discuss the optimization techniques which have been implemented for the proposed system.

III. APPLICATION OF OPTIMIZATION TECHNIQUES FOR AMB

A. GENETIC ALGORITHM (GA)

In the area of problem-solving, genetic algorithms (GA) have been used for almost four decades. In 1970, Holland was the first to propose the basic ideas of a Genetic Algorithm [33]. This pioneer idea of problem-solving was a substantial addition to scientific and engineering applications. Thanks to the work of scholars and engineers all across the world, GA development has reached a mature stage. It has grown rapidly as a result of the widespread availability of low-cost, high-speed tiny computers.

A genetic algorithm is an optimization approach that draws inspiration from the biological process of natural selection, in which the most adaptive and fit individuals succeed [34].

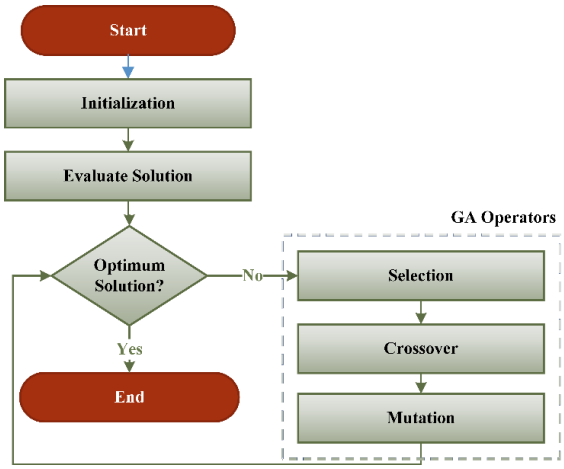

FIGURE 4. Flowchart of Genetic algorithm (GA).

Because of the GA's inherent properties, a genetic search may be well adapted to multi-objective optimization problems. A major characteristic is its multi-directional and global search, which is accomplished by keeping a population of potential solutions from generation to generation. It is a stochastic type nonlinear optimization technique. Adaptability, robustness, and flexibility are the three major advantages of the GA optimization technique [35]. Applications of GA are not limited, wherever a global search is required with a better robustness, GA is the very first choice for the researchers and engineers. Although, in literature, applications of GA are in pattern and system identification [36], [37], control [38], [39]& robotics [40], engineering designs [41], nonlinear system identification and optimization [42] and many more.

The GA has a few mathematical requirements for solving problems and can handle a wide range of objective functions and constraints. Because of their evolutionary character, GA can look for answers regardless of the inner working of the problem. Figure 4 shows a flowchart of GA optimization technique [43].

Genetic Algorithm optimization starts with defining the initial population which is basically a set of possible solutions in a finite range to the given objective function. Each element of the set is termed a 'chromosome' on which genetic operators (i.e., selection, crossover, and mutation) perform the optimization. Referring to Figure 4, after evaluation, if the optimum solution is not achieved then the selection operator begins to choose individuals for producing offspring based on their fitness score or, fitness value. The popular selection schemes are tournament selection, rank-based selection, roulette-wheel selection, etc. A comparison among these selection schemes is given in [44]. Individuals selected by the selection operator will go for crossover operation. This is the main variation operator which combines usually two individuals by exchanging some of their parts and generating offspring. Techniques to implement crossover operation are-single-point, n-point, uniform crossover, etc. The probability

per individual to go through the crossover is defined by the crossover probability (p_c), an externally derived parameter. The range of p_c is [0.6,1.0] [45]. The next step is mutation; it randomly alters each chromosome of offspring with a probability known as mutation probability (p_m). Value of p_m is typically less than 1% [46]. Greater the value of p_m will change the GA into a local search rather than a global search.

B. PARTICLE SWARM OPTIMIZATION (PSO) ALGORITHM

A stochastic-type method based on swarm intelligence is called particle swarm optimization (PSO). Kennedy and Eberhart introduced the PSO algorithm in their article in 1995 [47]. The genetic algorithm and PSO both are stochastic-type population-based algorithms. But PSO doesn't have genetic operators and the absence of this operator made it much more flexible and simpler. In PSO, all population members will participate and survive in the optimization process from the very beginning to the end [48].

The main feature of a swarm-intelligence-based algorithm is self-organization, a process in which an initial disorder populace (called a swarm) arranges itself in coordination only by local interaction between them and the learning experience of their own members [49]. Self-organization in birds, fish, insects, and herds is a natural behavior for searching for food, hunting, etc. Application of PSO is- renewable energy area [50], automation and control [51], medical [52] and biological engineering [53], operation research [54], and so forth. In a number of studies, the PSO algorithm has been shown to be a successful optimization technique. A relatively complete flowchart of the PSO algorithm is depicted in Figure 5 [47],

Explaining the flowchart mathematically, for a swarm size of n, in an M-dimensional space, the initial parameters are-

The position vector of particles (Y_i),

$$(Y_i) = (y_{i1}, y_{i2}, \ldots y_{im}, \ldots y_{iM})$$

The velocity vector of particles (V_i),

$$(V_i) = (v_{i1}, v_{i2}, \ldots v_{im}, \ldots v_{iM})$$

The optimal position of each particle (P_i),

$$(P_i) = (p_{i1}, p_{i2}, ..p_{im}, ..p_{iM})$$

The optimal position of swarm (P_g),

$$(P_g) = (p_{g1}, p_{g2}, \ldots p_{gm}, \ldots p_{gM})$$

At each position of the particle, the objective function is evaluated and then the particle position and velocity are updated by Equation 3 and Equation 4,

$$y^m_{i,t+1} = y^m_{i,t} + v^m_{i,t+1} \tag{3}$$

$$v^m_{i,t+1} = v^m_{i,t} + c_1 * r_1 * \left(p^m_{i,t} - y^m_{i,t}\right) + \left(c_2 * r_2 - \left(p^m_{g,t} - y^m_{i,t}\right)\right) \tag{4}$$

Here, c_1 = Cognitive parameters, c_2 = Social parameters, r_1 and r_2 are random numbers between 0 and 1. Subscript '$t+1$' shows the updated values and subscript 't' shows the current value. p^m_i and p^m_g are best-remembered individual's particle position and swarm position respectively.

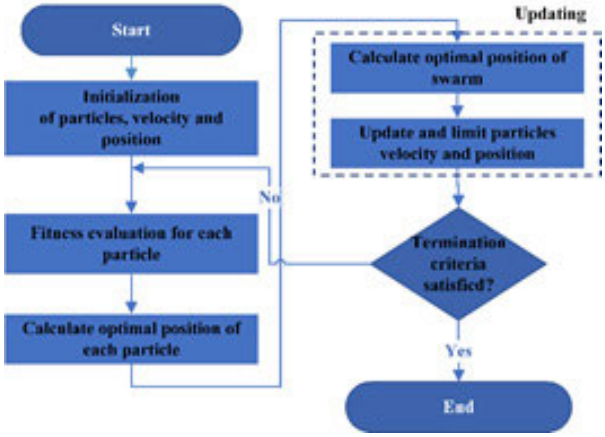

FIGURE 5. Flowchart representation of particle swarm optimization (PSO) algorithm.

C. CUCKOO SEARCH ALGORITHM (CSA)

Yang and Deb introduced the well-known optimization technique Cuckoo search (CS) in 2009 [55]. This metaheuristic algorithm mimics the brood breeding strategy of several species of cuckoo birds, together *Lévy* flight behavior of some [56]. Some cuckoo species lays their eggs in other bird nests at first. However, host birds may discover that these eggs are not their own (with a probability of p_a) and may either destroy or abandon them [57]. This indicates that the number of nests will decrease with each generation, thus it is believed that the hosting bird that abandoned his nest would establish a new nest in a different area therefore maintaining the number of nests constant between generations and introducing variation to the CS algorithm via fresh nest location [58].

In CSA, the random walk is based on *Lévy* flight which makes it most efficient from the perspective of performance and speed. There are various research fields in which cuckoo search algorithm has been implemented for optimization [59], [60]. The flowchart for CSA is depicted in Figure 6.

Newly generated cuckoo (x_i^{t+1}) using *Lévy* flight is given by,

$$x_i^{t+1} = x_i^t + \alpha \oplus Lévy\,(\lambda) \tag{5}$$

where, α is the step size which varies according to the problem and mostly $\alpha = 1$. The symbol $\oplus$ shows entry wise multiplication. The *Lévy* flight gives basically a random walk, with the random step length selected from an *Lévy* distribution. Equation 6 has infinite variance with an infinite mean.

$$Lévy \sim u = t^{-\lambda} \tag{6}$$

IV. RESULTS AND DISCUSSION

To implement any optimization technique, the basic requirement is to select an objective function. The variable of the

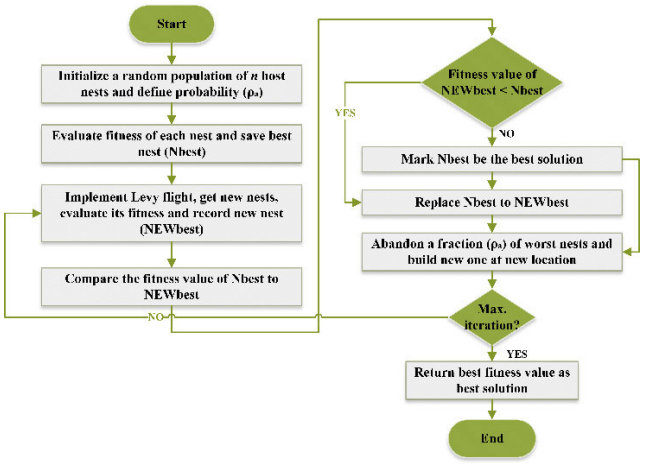

FIGURE 6. Flowchart representation of cuckoo search algorithm (CSA).

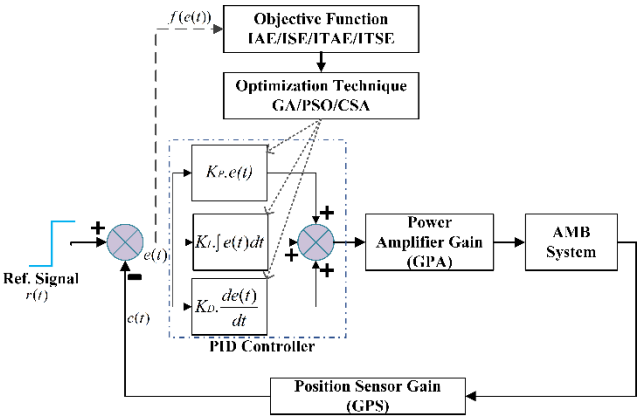

FIGURE 7. Implementation of optimization techniques in the AMB system.

objective function should have the ability to affect the closed-loop performance. In this manuscript, the gains of a PID controller (i.e., Proportional gain K_P, Integral gain (K_I) and Derivative gain (K_D)) are considered as variables. By changing the values of these variables, the error signal (difference between the reference signal and feedback signal) is tried to be minimized with the help of objective functions. Such that the closed loop's performance is steady and exhibits the fewest oscillations at its normal operating point.

$$e(t) = r(t) - y(t) \tag{7}$$

e(t) = Error Signal, r(t) is reference signal and y(t) is feedback signal.

Performance analysis is conducted using four objective functions with the use of three optimization techniques, the goal here is to reduce the error which is input to the controller. These four objective functions are-

1. Integral of absolute error (IAE)- It integrates the square of error over time.

$$\text{IAE} = \int_0^T |e(t)|\, dt \tag{8}$$

2. Integral of squared error (ISE)- IAE integrates the absolute error over time.

$$\text{ISE} = \int_0^T e^2\,(t)\, dt \tag{9}$$

3. Integral of time multiplied absolute error (ITAE)- ITSE integrates the square of the error multiplied with time over time.

$$\text{ITAE} = \int_0^T t\,|e(t)|\, dt \tag{10}$$

4. Integral of time multiplied squared error (ITSE)- ITAE integrates the absolute error multiplied by the time over time.

$$\text{ITSE} = \int_0^T t.\left(e^2(t)\right) dt \tag{11}$$

The above objective functions are implemented in optimization methods to calculate the gains values of the PID controller as shown in Figure 7. These gains are then fed to the PID controller to maintain the close loop stable, at the equilibrium point of operation.

TABLE 2. Required initialization parameters for genetic algorithm.

S No.	Required Parameters	Representation	Assumed Value
1.	Population size	N	50
2.	Number of iterations	T	100
3.	Minimum limit of gain parameters	lb	[0,0,0]
4.	Maximum limit gain parameters	ub	[10,100,0.15]

The proposed system is briefed in section II of this manuscript. The linearized transfer function at the normalized operating point (Equation 2) is implemented in a closed-loop form with a PID controller as shown in Figure 7. The reference signal r(t) is a unit step signal which is compared by the feedback signal c(t) (having numerical value) and generates an error signal e(t). The objective functions chosen in this paper are based on the error profile of the system. The error signal value is then implemented in these objective functions (IAE, ISE, ITAE, and ITSE), and using different optimization techniques PID controller gains are calculated (for the proposed AMB system at a nominal operating point).

A. IMPLEMENTATION OF GENETIC ALGORITHM (GA)

Several parameters must be defined during the GA initialization procedure, and those parameters, along with their assumed values for optimization, are listed in Table 2.

The gain parameters of the PID controller for the proposed closed-loop system are computed using the parameters listed in Table 2 by running the genetic algorithm separately for four different objective functions. The optimized gain parameters have been achieved and are shown in Table 3.

A transfer function is formed for each objective function using the gain parameters value. Utilizing these controller transfer functions with the AMB transfer function (Equation 2) in a closed loop and by applying a unit step signal (for a duration of 0.15sec), its response on a proposed closed loop

TABLE 3. PID gain parameters value optimized by GA technique.

Sl. No	Optimization method	Objective function	K_p	K_I	K_D	$\frac{s^2K_D + sK_p + K_I}{s}$
1.	GA	IAE	4.853	50.595	0.0838	$\frac{0.0838s^2 + 4.853s + 50.595}{s}$
		ISE	5.952	59.781	0.0931	$\frac{0.0931s^2 + 5.952s + 59.781}{s}$
		ITAE	4.533	67.978	0.0872	$\frac{0.0872s^2 + 4.533s + 67.978}{s}$
		ITSE	6.318	80.035	0.1072	$\frac{0.1072s^2 + 6.318s + 80.035}{s}$

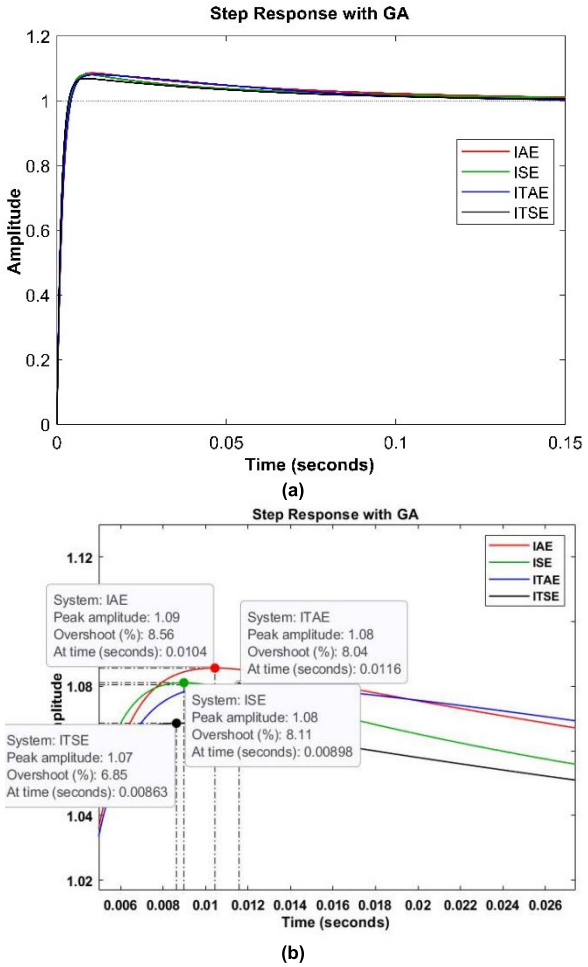

FIGURE 8. (a) Unit step response of proposed closed-loop system realized by enforcing GA, (b) Magnified for duration 0.006sec-0.026sec.

is observed as depicted in Figure 8(a). A tighter step response plot with overshoot values over the time of 0.006sec-0.026sec is depicted in Figure 8(b).

Transient state parameters and phase margin have been evaluated and are presented in Table 4 with the help of the step response depicted in Figure 8. where, E_{ss} is steady state error, J is the final value of the objective function and P.M is phase

TABLE 4. Using GA technique -time domain analysis parameters, final value of performance indies and phase margin values.

Sl. No	Optimization method	Objective function	$\%M_p$	t_r (sec)	t_p (sec)	t_s (sec)	E_{ss}	J	$P.M$ (In degree)
1.	GA	IAE	8.90	0.00241	0.01040	0.07028	0.001	1.0090	84.8
		ISE	8.11	0.00249	0.00898	0.09201	0.001	1.0080	84.9
		ITAE	8.05	0.00270	0.01160	0.08282	0.001	0.5040	85.5
		ITSE	6.85	0.00220	0.00863	0.07777	0.001	0.5040	85.9

TABLE 5. Initialization parameters for PSO algorithm.

S No.	Required Parameters	Representation	Assumed Value
1.	Swarm Size	N	50
2.	Number of iterations	T	100
3.	Minimum limit of gain parameters	lb	[0,0,0]
4.	Maximum limit gain parameters	ub	[10,100,0.15]

margin in degree, $\%M_P$ is percentage peak overshoot, t_r, t_p, t_s are rise, peak, and settling times in seconds respectively.

Data of transient state parameters listed in Table 4 shows that ITSE objective function has minimum value $\%M_p$, t_r and t_p of as compared to other objective functions. This results in a faster and smoother control of the proposed system.

To analyze the stability of the proposed closed loop with GA optimized PID controller, bode plot is obtained as depicted in Figure 9 and Table 4 shows that ITSE objective function has maximum value of phase margin which represents a wide control region for the system.

For further analysis, the root locus plot and Nyquist plot are observed as shown in Figure 10. Depending upon the open loop transfer function of the controller along with the proposed system and feedback gain of position sensor root locus plot is obtained for different objective functions. The stability of the system is further verified with the help of the Nyquist plot. Here, for all of the objective functions, $(-1,0)$ coordinate is encircled in anticlockwise direction. Which confirms that the closed loop system is stable.

The genetic algorithm with ITSE objective function shows almost the fastest and smoothest step response for the proposed system.

B. IMPLEMENTATION OF PARTICLE SWARM OPTIMIZATION (PSO)

For three-dimensional space, the initial parameters required for the execution of the PSO algorithm with their assumed values are placed in Table 5.

The algorithm is executed using the flowchart shown in Figure 5. After the completion gains the value of the PID controller is obtained which is listed in Table 6 in conjunction with the controller transfer function.

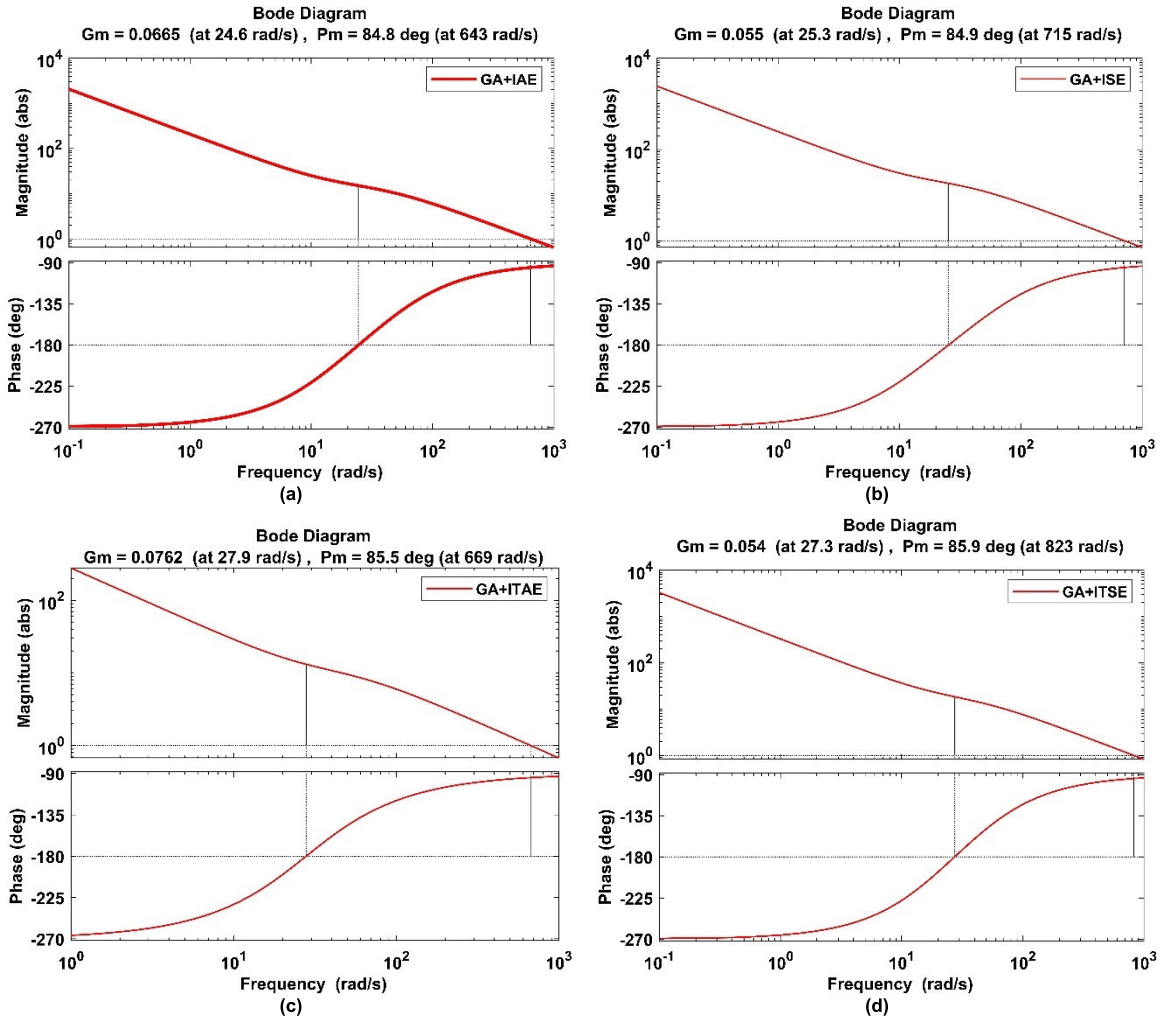

FIGURE 9. Bode plot with gain margin and phase margin values of (a) GA-IAE (b) GA-ISE (c) GA-ITAE and (d) GA-ITSE.

TABLE 6. PID gain parameters value optimized by PSO technique.

Sl. No.	Optimization method	Objective function	K_P	K_I	K_D	$\frac{s^2K_D + sK_p + K_I}{s}$
1	PSO	IAE	4.234	54.213	0.0801	$\frac{0.0801s^2 + 4.234s + 54.21}{s}$
		ISE	9.931	67.676	0.1087	$\frac{0.1087s^2 + 9.931s + 67.67}{s}$
		ITAE	4.157	62.428	0.0837	$\frac{0.0837s^2 + 4.157s + 62.42}{s}$
		ITSE	4.865	93.032	0.0980	$\frac{0.0980s^2 + 4.865s + 93.03}{s}$

TABLE 7. Using PSO technique -time domain analysis parameters, final value of performance indies, and phase margin.

Sl. No.	Optimization method	Objective function	$\%M_p$	t_r (sec)	t_p (sec)	t_s (sec)	E_{ss}	J	$P.M$ (In degree)
1.	PSO	IAE	8.72	0.002 91	0.011 9	0.10 10	0.0 01	1.0 090	85.1
		ISE	8.56	0.002 07	0.006 6	0.05 53	0.0 01	1.0 080	83.8
		ITAE	8.25	0.002 83	0.012 8	0.09 32	0.0 01	0.5 040	85.6
		ITSE	7.16	0.002 47	0.011 9	0.07 53	0.0 01	0.5 040	86.2

Similar to GA, here again to the proposed system a unit step signal of 0.15sec duration is applied and step response is realized as shown in Figure 11 with cramped step response of duration 0.004sec-0.018sec.

Time domain analysis is carried out on the step response and its parameters are calculated which are listed in Table 7.

For the above Table 7, it is realized that the ITSE objective function has the least overshoot with the second-best rise time. Other than ITSE the peak overshoot of the remaining objective function is almost the same but with ISE rise time is minimum. From the phase margin value, it is clear that ITSE shows the greatest stability region. The Bode plot for these objective functions with the detailed value of gain margin and phase margin is depicted in Figure 12.

For various objective functions, a root locus plot is created based on the controller's open loop transfer function and the proposed system.

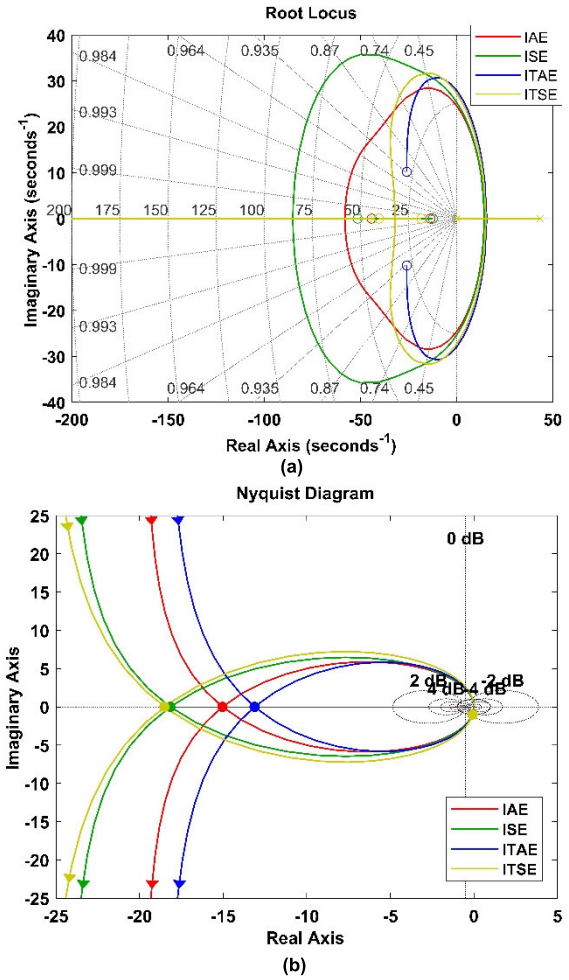

FIGURE 10. Enforcing GA with objective functions- (a) root locus plot, (b) Nyquist Plot.

TABLE 8. Initialization parameters of cuckoo search algorithm.

S No.	Required Parameters	Representation	Assumed Value
1.	Number of host nests	N	50
2.	Number of iterations	T	100
3.	Minimum limit of gain parameters	lb	[0,0,0]
4.	Maximum limit gain parameters	ub	[10,100,0.15]

The system's stability is validated using the Nyquist plot. In this case, the $(-1,0)$ coordinate is wrapped in an anticlockwise orientation for all objective functions. This validates the closed-loop system's stability. Both the root locus plot and Nyquist plot is shown in Figure 13.

From the perspective of time domain analysis and phase margin, it is evident that PSO-ITSE has a better and more stable performance.

C. IMPLEMENTATION OF CUCKOO SEARCH ALGORITHM (CSA)

The initialization of the cuckoo search algorithm requires a few parameters, which are provided in Table 8.

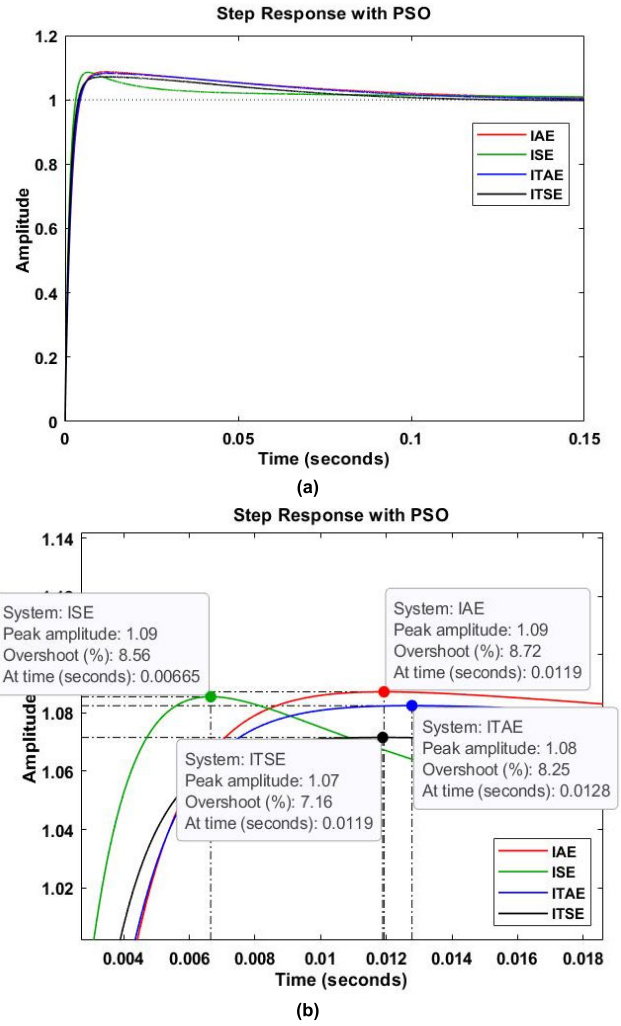

FIGURE 11. (a) Unit step response of proposed closed-loop system realized by enforcing PSO, (b) Magnified for duration 0.004 sec - 0.018 sec.

TABLE 9. PID gain parameters value optimized by CSA technique.

Sl. No	Optimization method	Objective function	K_p	K_I	K_D	$\frac{s^2K_D + sK_p + K_I}{s}$
1.	CSA	IAE	3.895	62.873	0.0873	$\frac{0.0873s^2 + 3.895s + 62.873}{s}$
		ISE	5.252	61.908	0.0935	$\frac{0.0935s^2 + 5.252s + 61.908}{s}$
		ITAE	5.554	67.966	0.0998	$\frac{0.0998s^2 + 5.554s + 67.966}{s}$
		ITSE	6.794	85.251	0.1117	$\frac{0.1117s^2 + 6.794s + 85.251}{s}$

For PID controller the gain parameters i.e., K_P, K_I and K_D are calculated using flowchart of CSA shown in Figure 6 for four different objective functions and the realized values are shown in Table 9.

The PID controller transfer function from Table 9 is used in a closed loop form with the proposed system, and a step signal of unit amplitude for 0.15sec is given as input to the system.

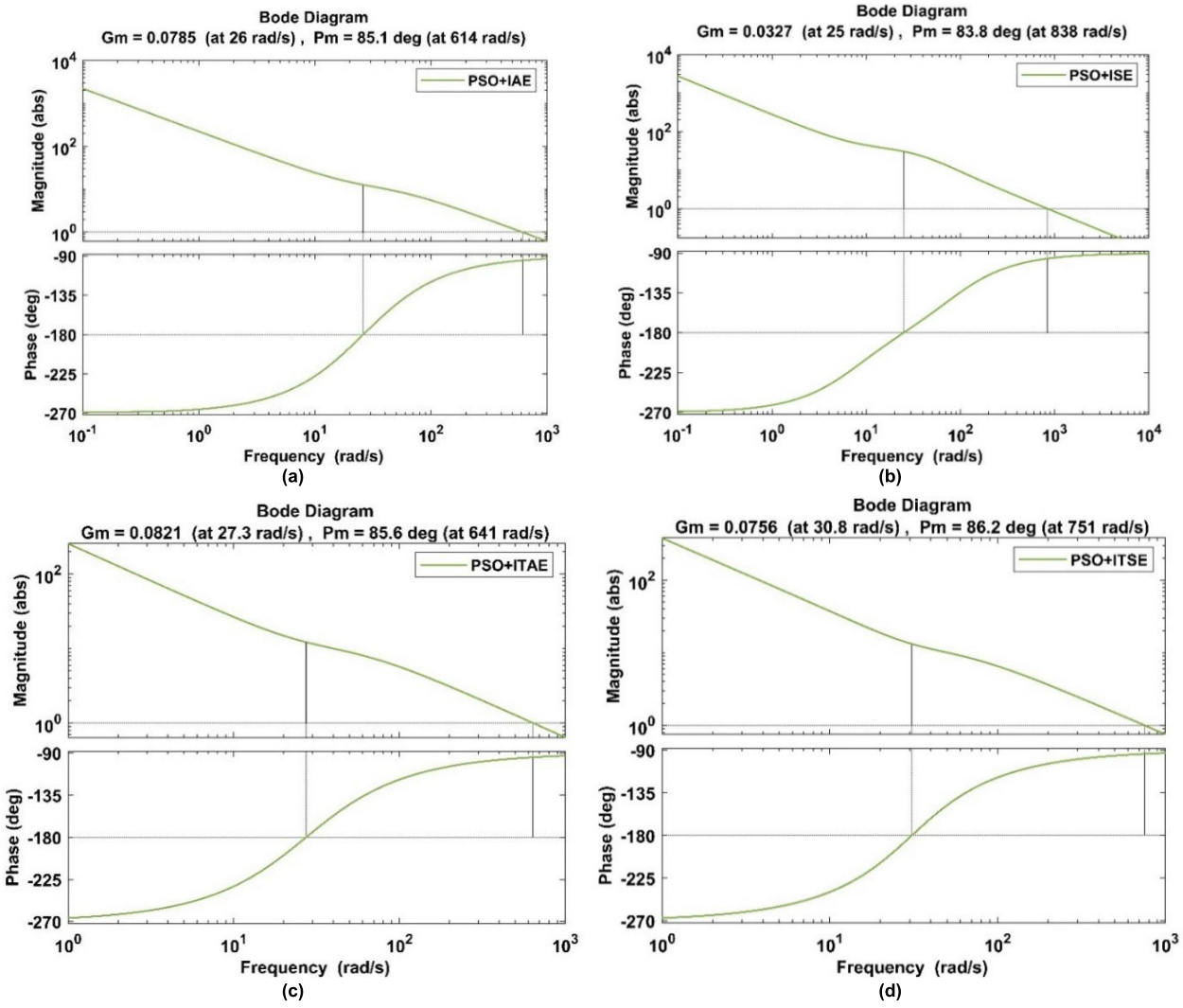

FIGURE 12. Bode plot with gain margin and phase margin values of (a) PSO-IAE (b) PSO-ISE (c) PSO-ITAE and (d) PSO-ITSE.

This yields the suggested system's step response, as shown in Figure 14(a), and a closer step response with a duration of 0.005sec-0.022sec is also displayed in Figure 14(b).

The goal of charting step response is to acquire and evaluate the time domain behavior of a closed loop system with optimum PID controller gain settings. Table 10, displays all of the transient state characteristics of the proposed system, as well as the goal function value and phase margin.

Table 10, shows that ITSE has the least overshoot with a faster rising and settling time, followed by the ITAE objective function. The performance of the IAE and ISE objective functions is nearly identical, with a little variance in peak overshoot and settling time. In this case, the phase margin of the ISE objective function is greater than that of the other objective functions. However, ITSE has still the best overall performance. Figure 15 shows a bode plot with the value of the gain margin and phase margin of the CSA algorithm with all goal functions.

TABLE 10. Time domain analysis parameter, final value of objective function and phase margin with CSA.

Sl. No	Optimization method	Objective function	$\%M_p$	t_r (sec)	t_p (sec)	t_s (sec)	E_{ss}	J	$P.M$ (in degree)
1	Cuckoo Search Algorithm (CSA)	IAE	7.72	0.002 81	0.016 80	0.09 54	0.0 01	1.00 90	86.2
		ISE	7.62	0.002 52	0.009 92	0.09 36	0.0 01	1.00 80	85.5
		ITAE	7.12	0.002 39	0.009 55	0.08 85	0.0 01	0.50 45	85.8
		ITSE	6.69	0.002 14	0.008 16	0.07 31	0.0 01	0.50 40	85.9

A root locus plot is generated for each goal function based on the controller's open loop transfer function and the proposed system.

The Nyquist plot is used to assess the system's stability. For all objective functions, the $(-1,0)$ coordinate is enclosed in an anticlockwise direction. This confirms the stability of the closed-loop system. Figure 16 shows both the root locus plot and the Nyquist plot.

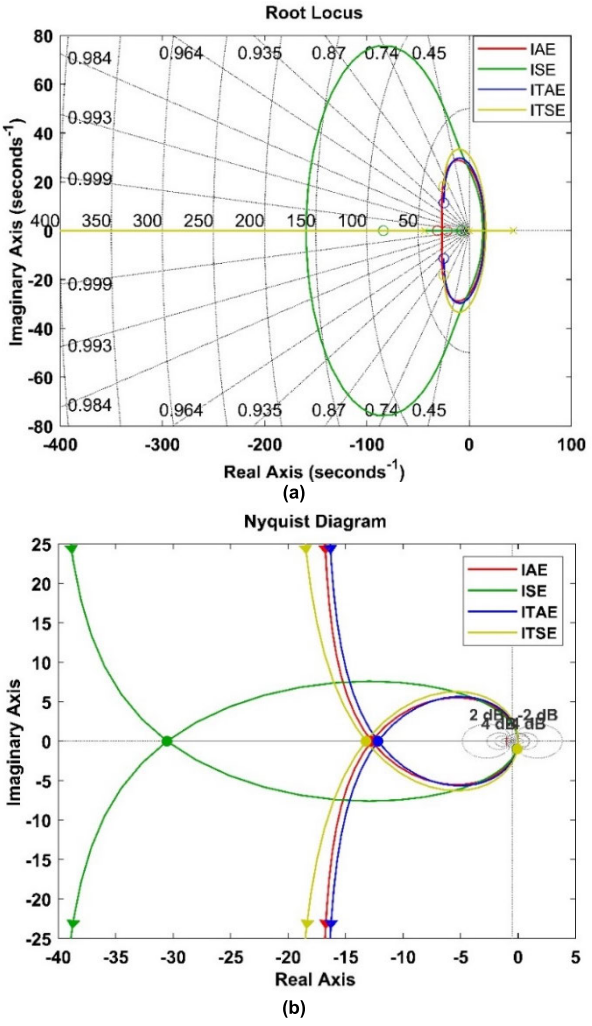

FIGURE 13. Enforcing PSO with objective functions- (a) root locus plot, (b) Nyquist Plot.

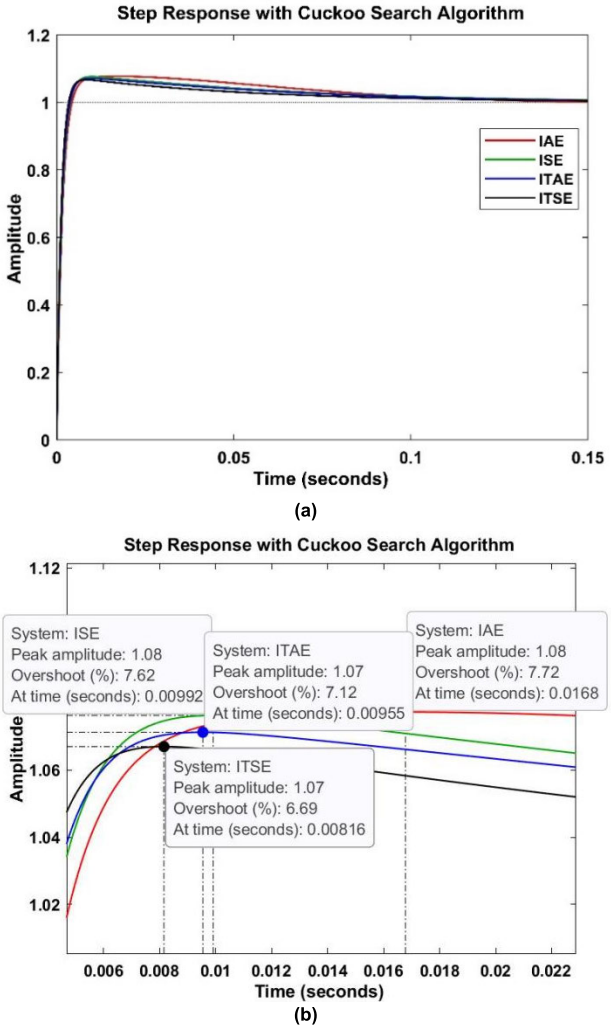

FIGURE 14. (a) Unit step response of proposed closed-loop system realized by enforcing CSA, (b) Magnified for duration, 0.006 sec - 0.022 sec.

Here, again among all of the objective functions ITSE shows a better performance. Further in this paper, on the basis of statistical information of algorithm, time domain analysis, phase margin, and algorithm execution time, the performance of these optimization strategies with various objective functions is compared.

V. PERFORMANCE EVALUATION OF ALGORITHMS USING VARIOUS OBJECTIVE FUNCTIONS FOR GA, PSO, AND CSA

For a fair comparison among these three optimization techniques. All of the algorithms are executed for 100 number of iterations for four different objective functions. Figure 17 shows how the value of the goal function varies with the number of iterations. Minimum limit maximum limit of gain parameters and major factor of algorithm (swarm size for PSO, no. of host nests for CSA and population for GA) is kept equal.

The calculated values of the objective function for all objective functions in the CSA and GA algorithms reduce as the number of iterations rises. In contrast, using the PSO method, the objective function value drops for a period of time until being saturated at the optimized value.

1) BASED ON INFORMATION FROM STATISTICAL ANALYSIS

The scientific method of statistical analysis enables us to deepen our comprehension of data analysis and draw out pertinent information from readily available data. In this work, the statistically performance of the algorithms is observed and analyzed. Data of several statistical parameters- mean, standard deviation, and variance, are collected and displayed in Table 11- Table 13. In addition, for 100 iterations, the objective function's minimal highest, and the difference between minimal and highest values are realized and recorded.

En bloc, data from Table 11-Table 13 are analyzed and a comparison is observed as illustrated in Figure 18.

The main objective is to gain a complete understanding of how statistical data parameters evolve over time. Here, Mean - displays the objective function's ultimate value, and it is evident from Figure 18(a) that the IAE, followed by the

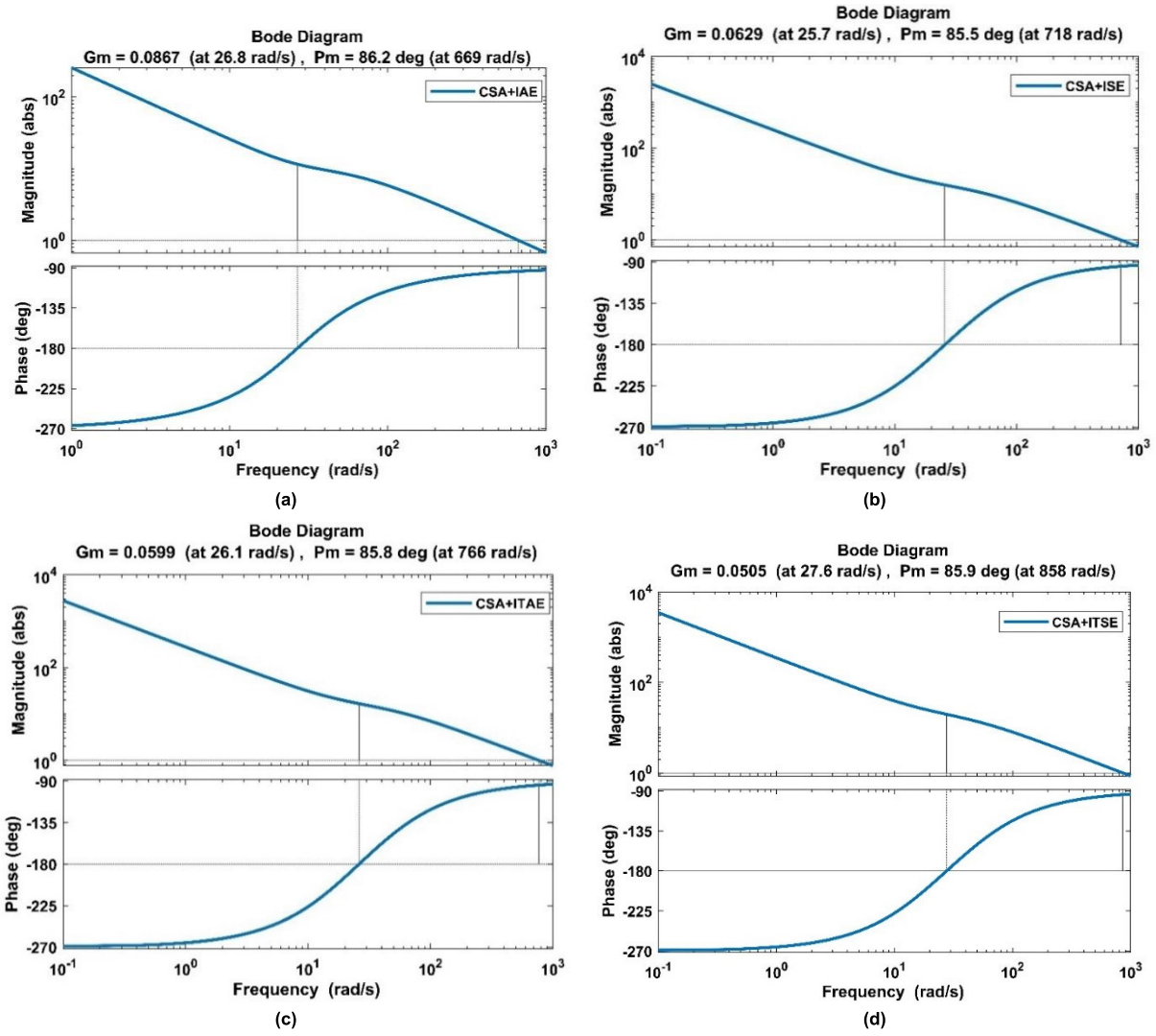

FIGURE 15. Bode plot with gain margin and phase margin values of (a) CSA-IAE (b) CSA-ISE (c) CSA-ITAE and (d) CSA-ITSE.

ISE, offers the objective function's greatest value. On the other hand, ITSE enhances and drastically lowers the value of the objective function. The second-best minimal value of the objective function is provided by the ITAE objective function.

The amount of statistical dispersion of data points analogous to its mean is defined as standard deviation. Mathematically, the standard deviation is the square root of variance. Both of these measures demonstrate variability in data distribution. In this analysis, the standard deviation and variance data comparison plot is illustrated in Figure 18(b) and Figure 18(c) respectively.

2) BASED ON INFORMATION COLLECTED FROM PHASE MARGIN AND TRANSIENT STATE ANALYSIS

The proposed closed-loop system's stabilization is the main objective of this work to ensure smooth and effective bearing functioning. Transient state analysis may be used to assess how well the suggested closed loop functions and observations on stability can be made by looking at the phase margin of the system. The values of several transient state parameters, including peak overshoot, rising time, peak time, and

TABLE 11. Statistical analysis data of genetic algorithm.

Sl. No.	Parameters	GA-IAE	GA-ISE	GA-ITAE	GA-ITSE
1.	Mean	1.00899055	1.0079821	0.504492790	0.5039860898
2.	Standard Deviation	2.162614e-08	4.32032e-08	3.3855474e-09	6.7643186e-09
3.	Variance	4.676903e-16	1.8665165e-15	1.1461931e-17	4.5756007e-17
4.	Minimal value of objective function	1.008990465	1.0079819506	0.504492783	0.50398607678
5.	Highest value of objective function	1.008990579	1.0079821777	0.504492793	0.50398609634
6.	Difference	1.1367475e-07	2.2710165e-07	9.7897445e-09	1.9559977e-08

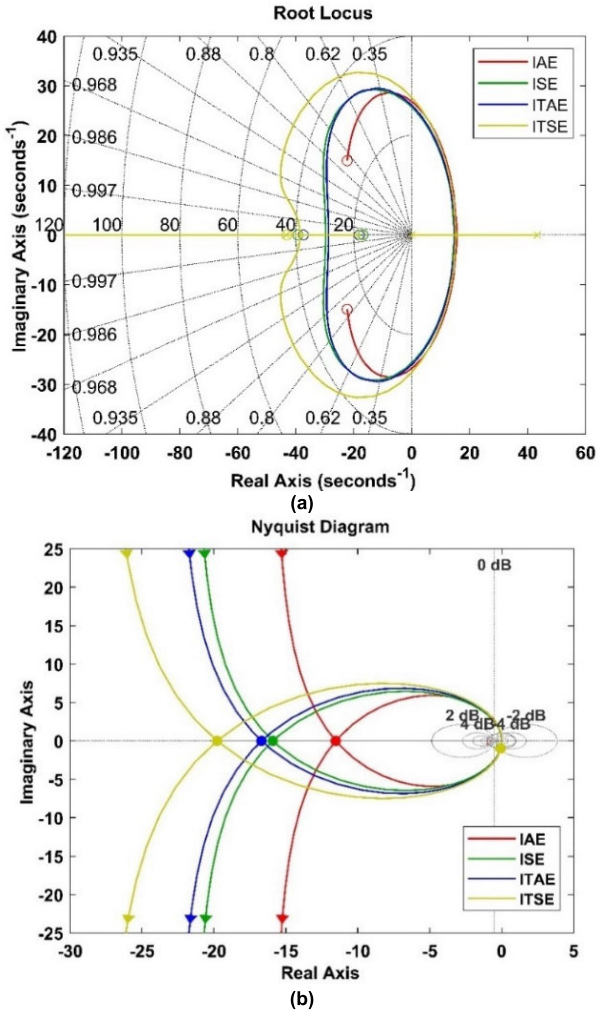

FIGURE 16. Enforcing CSA with objective functions- (a) root locus plot, (b) Nyquist Plot.

TABLE 12. Statistical analysis data of particle swarm optimization.

Sl. No.	Parameters	PSO-IAE	PSO -ISE	PSO -ITAE	PSO -ITSE
1.	Mean	1.00899257	1.00798625	0.504493984	0.503988495
2.	Standard Deviation	1.840391e-07	3.286449e-07	2.926953e-08	1.069017e-07
3.	Variance	3.387040e-14	1.080074e-13	8.5670590e-16	1.142799e-14
4.	Minimal value of objective function	1.00899249	1.00798602	0.504493975	0.503988458
5.	Highest value of objective function	1.00899353	1.00798718	0.504494191	0.503989157
6.	Difference	1.0410741e-06	1.1845718e-06	2.1553371e-07	6.9826652e-07

settling time, for the proposed system with various optimization strategies are shown in Tables 4, Table 7, and Table 10. A comparison is made using these transient state and phase margin information, as shown in Figure 19.

TABLE 13. Statistical analysis data of cuckoo search algorithm.

Sl. No.	Parameters	CSA-IAE	CSA -ISE	CSA -ITAE	CSA -ITSE
1.	Mean	1.008995355	1.007992416	0.504494267	0.503989442
2.	Standard Deviation	7.760993e-07	1.291511e-06	5.6140429e-07	7.3245547e-07
3.	Variance	6.023301e-13	1.668001e-12	3.151747e-13	5.3649102e-13
4.	Minimal value of objective function	1.00899387	1.00798924	0.50449279	0.503986922
5.	Highest value of objective function	1.00899670	1.00799438	0.50449483	0.503990021
6.	Difference	2.8343773e-06	5.1469575e-06	2.0428509e-06	3.2870064e-06

TABLE 14. Algorithm execution time for 100 iterations.

Sl. No.	Algorithm	Objective functions	Execution time (in seconds)
1.	Genetic Algorithm	IAE	224.9414
		ISE	264.2685
		ITAE	250.9672
		ITSE	254.5149
2.	Particle Swarm Optimization	IAE	220.7709
		ISE	274.9573
		ITAE	267.6009
		ITSE	275.4985
3.	Cuckoo Search Algorithm	IAE	86.0990
		ISE	69.1076
		ITAE	125.7139
		ITSE	82.4652

For an AMB system, the required features for designing a controller are less vibration, faster response, and a large stability region. Here, in Figure 19(a) from the comparison it is observable that CSA-ITSE has a minimum value of peak overshoot followed by GA-ITSE and then CSA-ITAE. The lesser the value of peak overshoot smaller will be the yank at the nominal point of operation. Therefore, CSA-ITSE will be the best choice among the other optimization techniqueobjective function combinations.

In a closed loop response of the controller must be rapid. This response comprises rise time, peak time, and ultimately the observation is made on the value of settling time. Smaller the value of settling time faster the response of the system. It may observe from Figure 19(b), Figure 19(c), and Figure 19(d) that PSO-ISE and GA-ITSE have a minimum value of rising time followed by CSA-ITSE. PSO-ISE has the smallest value of peak time and settling time. GA-IAE has the second-best peak and settling time and CSA-ITSE has the third-smallest peak and settling time.

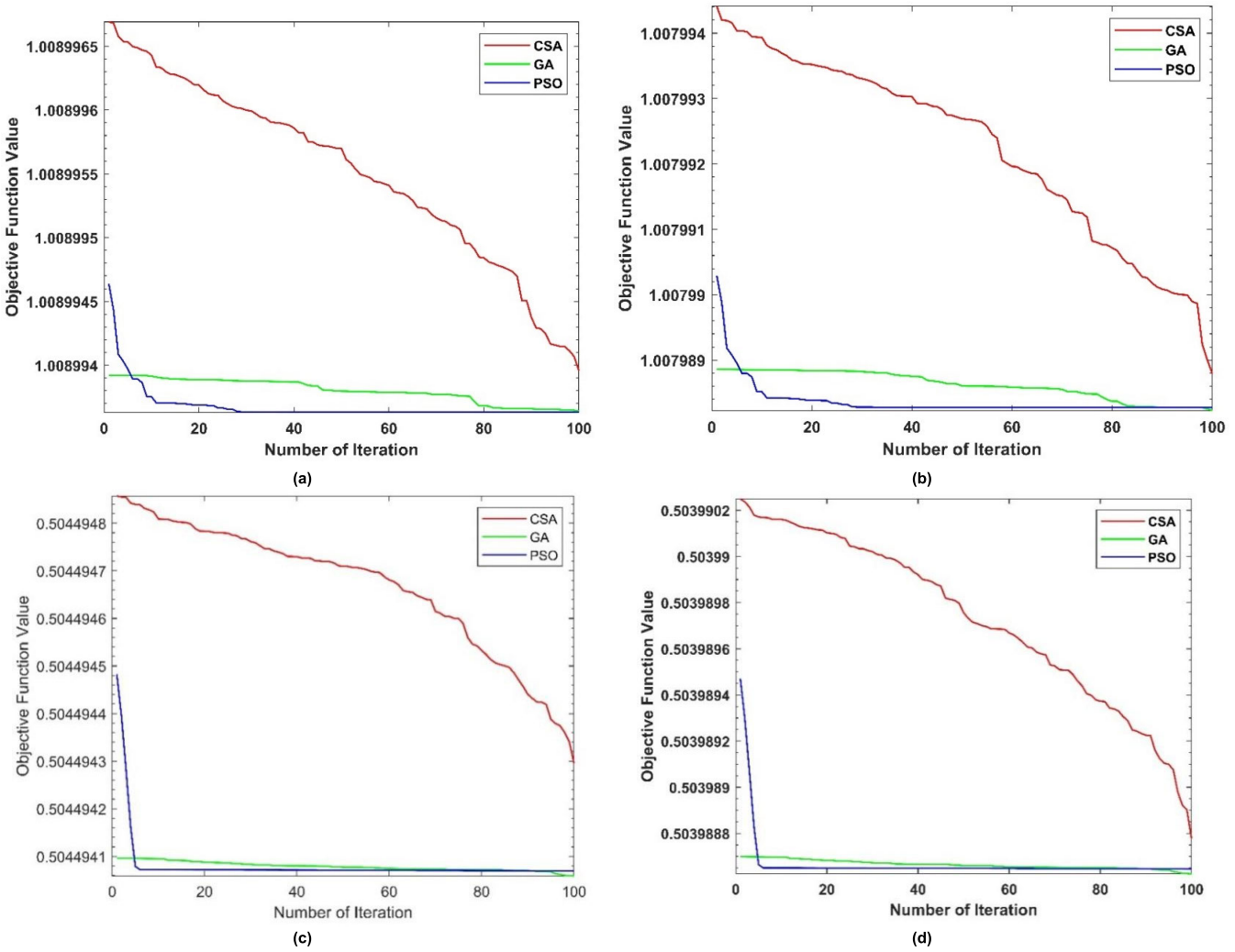

FIGURE 17. GA, PSO and CSA optimized objective function value (a) IAE, (b) ISE, (c) ITAE, and (d) ITSE, for 100 no. of iterations.

Apart from peak overshoot and speed of response, stability is also a major factor from the perspective of controller design. The larger the value of the phase margin denotes the wider the stability region. From Figure 19(e) it is clear that CSA-IAE and PSO-ITSE have a maximum value of phase margin followed by CSA-ITSE and GA-ITSE.

3) BASED ON THE DURATION OF AN ALGORITHM'S EXECUTION

Time taken by the algorithm to produce the desired outcome depends on various factors like objective function, system configuration, the complexity of the closed loop, no. of iterations, etc. In this article, a performance comparison of optimization techniques is carried out by assuming that all system and environmental factors are identical.

Execution time for optimization techniques with respect to the objective function for 100 no. of iteration is listed in Table 14 and the corresponding plot is depicted in Figure 20.

Minimum algorithm execution time is taken by CSA followed by GA and then PSO. Among the optimization technique-objective function combination, CSA-IAE took minimum time and then CSA-ITSE.

VI. CONCLUSION

The linearized transfer function of the proposed AMB system is unstable, requiring the inclusion of a PID controller in a closed loop for stable bearing operation. The gains of the PID controller play an important role in making the closed loop stable, and they may be computed using either traditional methods or intelligent optimization approaches. In this study, the gain values of the controller are estimated utilizing three distinct optimization strategies (GA, PSO, and CSA) with four different goal functions (IAE, ISE, ITAE, and ITSE). Statistically, the performance of each optimization technique with every objective function is obtained. Further, time domain analysis and frequency response analysis of the proposed closed loop is calculated. Later, the algorithm execution time for 100 no of iterations is obtained. From comparing these data, it is found that-

- The lowest value of the objective function is obtained by ITSE and then ITAE objective function.

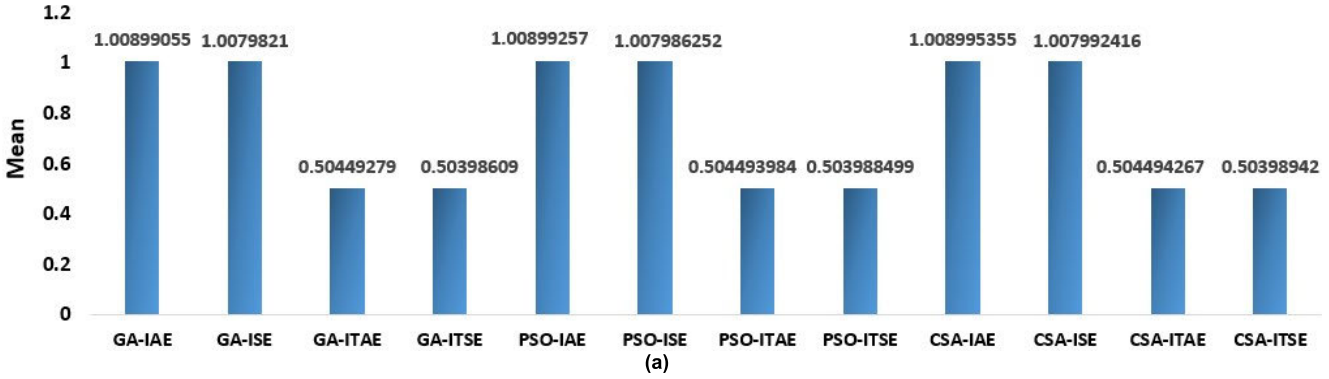

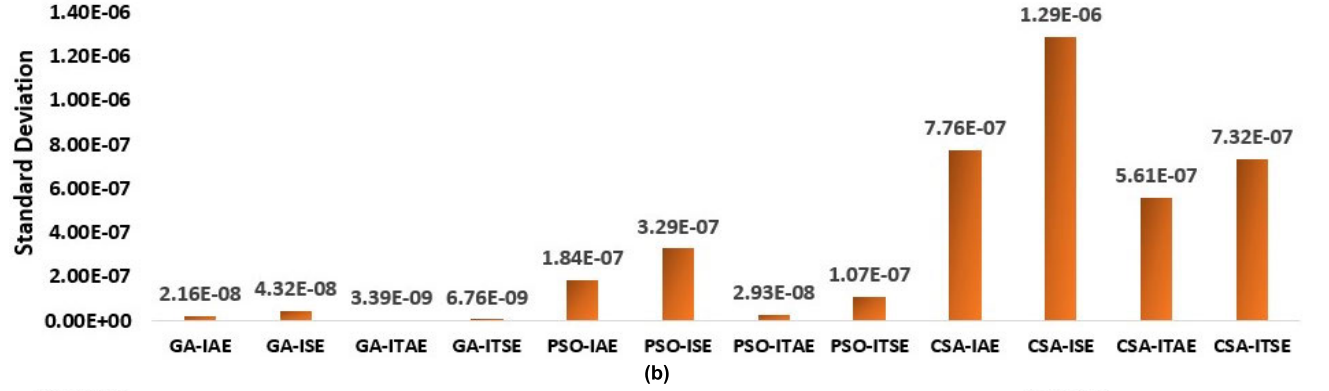

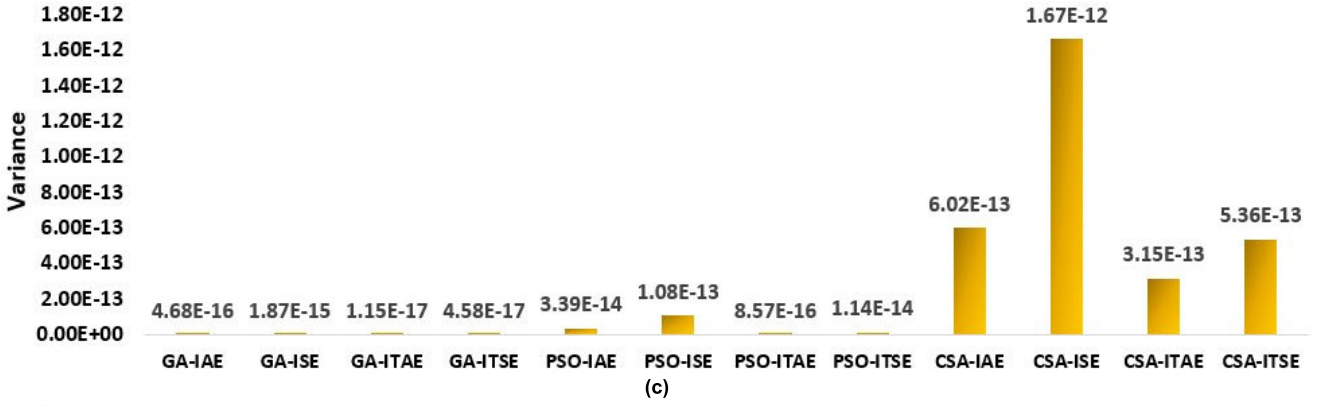

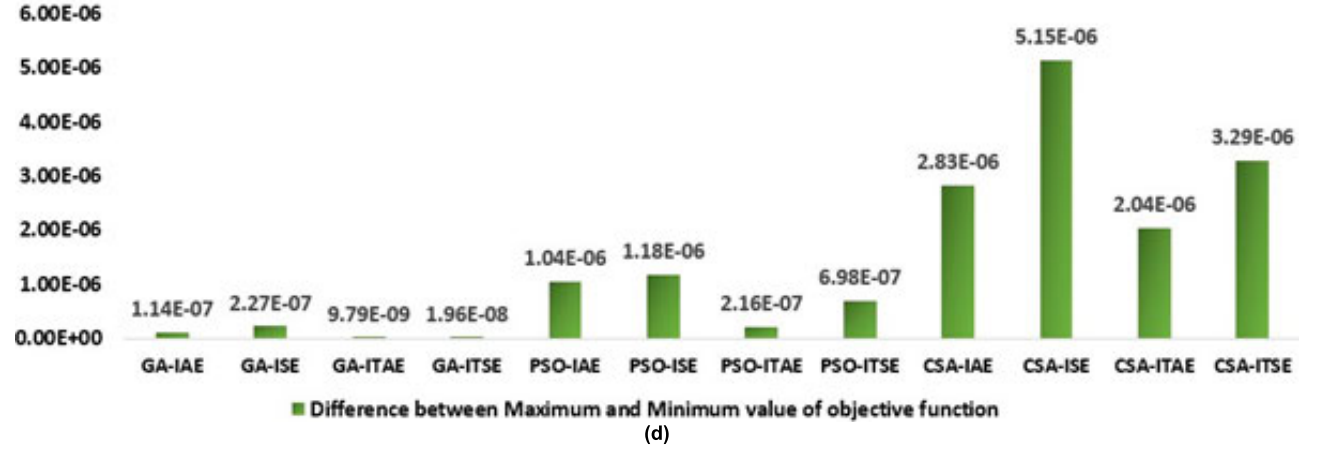

AQ:5 **FIGURE 18.** Computation based on information of statistical analysis (for 100 no of iterations): (a) Mean, (b) Standard deviation, (c) Variance and (d) Difference between highest and minimal value of objective function.

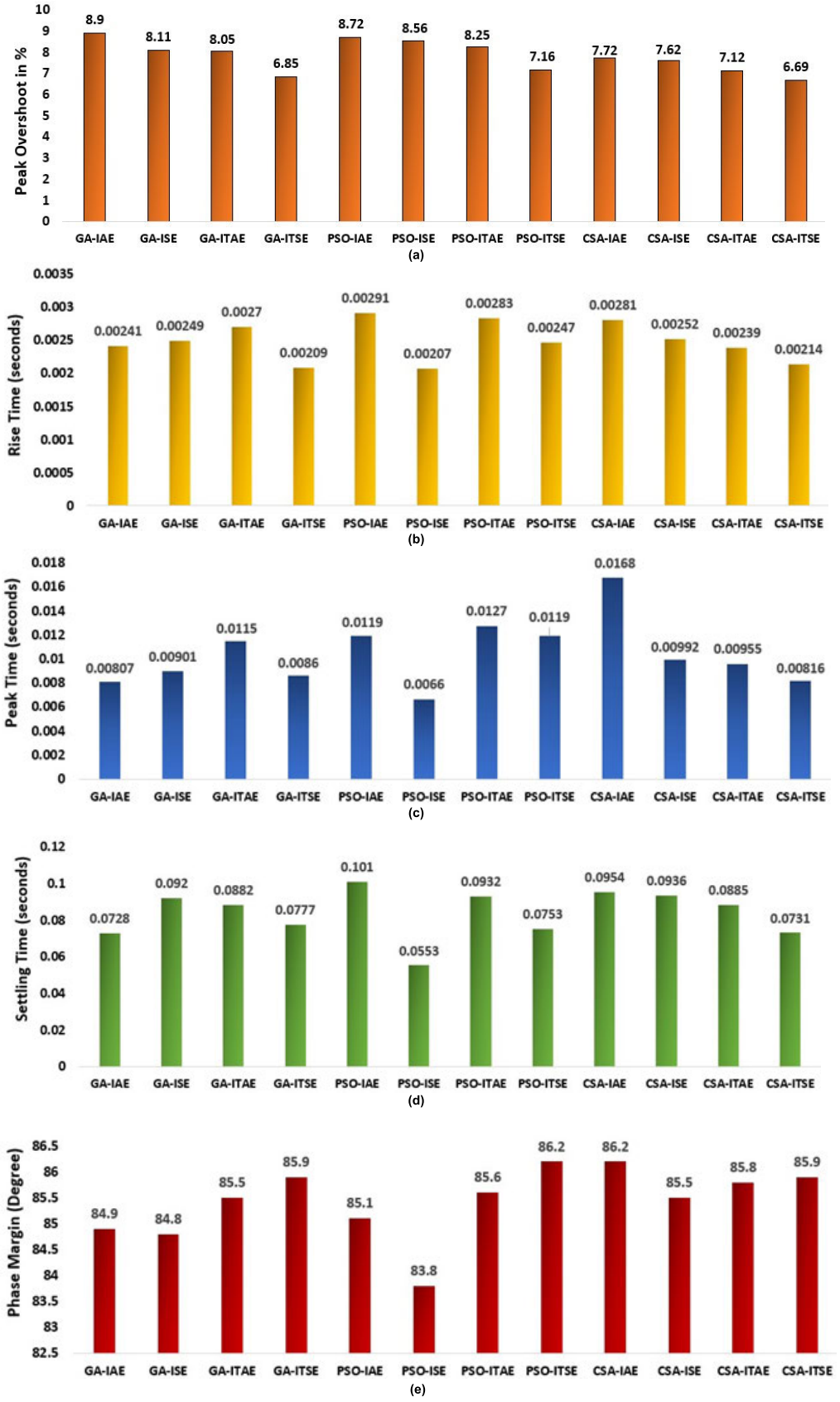

FIGURE 19. Comparative inspection of time domain analysis data: (a) Peak overshoot (%), (b) Rise time (in seconds), (c) Peak time (in seconds), (d) Settling time (in seconds) and (e) Phase Margin (in degree)).

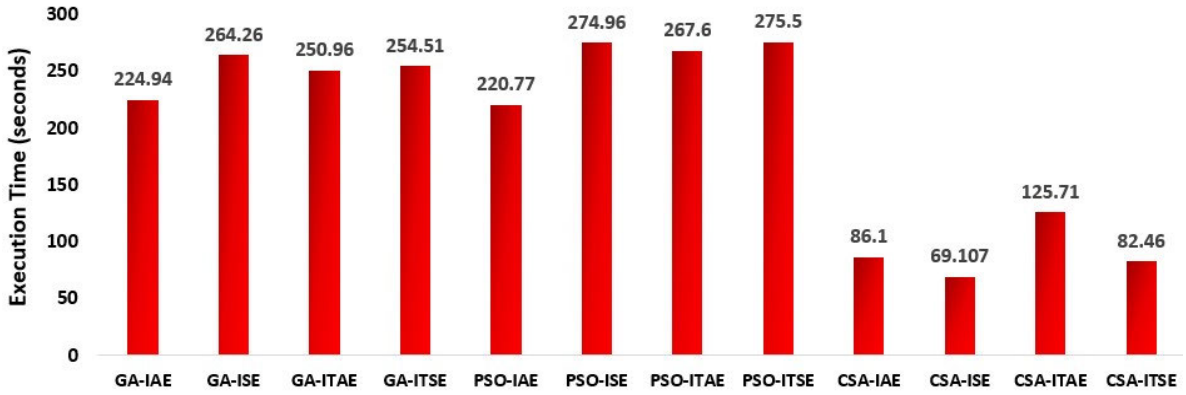

FIGURE 20. Algorithm execution time for 100 iterations.

- Parameters of time domain and frequency response analysis show that minimum peak overshoot is acquired by ITSE whereas the fastest response time is shown by PSO-ISE and then optimization techniques with ITSE objective function.
- CSA-ISE, followed by CSA-ITSE, takes the shortest amount of time to execute an algorithm.

The choice of optimization strategies and objective functions in terms of their effectiveness and efficiency is well illustrated by this comparative study analysis. An application where better closed-loop response along with quick controlling is essential, ITSE objective function optimized by cuckoo search algorithm will be a smart choice.

Although the metaheuristic optimization techniques are capable to provide improved control of the active magnetic bearing system as compared to conventional controlling methods. But by considering other innovative Artificial intelligence-based controlling strategies like deep neural network-based model predictive control tactics, the overall performance of the proposed system can be further improved in real-time.

With the help of the observation made in this manuscript. The effectiveness and applicability of GA, PSO, and CSA are studied which can be further used in such complex systems like electric vehicles (EVs), flywheel energy storage systems, and many more.

CONFLICT OF INTEREST

The authors declare no conflicts of interest to disclose.

REFERENCES

[1] G. Schweitzer, H. Bleuler, and A. Traxler, "Basics, properties and applications of active magnetic bearings," *Act. Magn. Bearings*, vol. 210, pp. 1–112, Jan. 1994.
[2] P. K. Sinha, *Electromagnetic Suspension: Dynamics and Control*. Stevenage, U.K.: Peregrinus, 1987.
[3] G. Schweitzer and E. H. Maslen, *Magnetic Bearings: Theory, Design, and Application to Rotating Machinery*, vol. 1. Berlin, Germany: Springer, 2009.
[4] G. Schweitzer, "Mechatronics—A concept with examples in active magnetic bearings," *Mechatronics*, vol. 2, no. 1, pp. 65–74, Feb. 1992.
[5] H. Hoshi, T. Shinshi, and S. Takatani, "Third-generation blood pumps with mechanical noncontact magnetic bearings," *Artif. Organs*, vol. 30, no. 5, pp. 324–338, May 2006.
[6] T. Akamatsu, T. Nakazeki, and H. Itoh, "Centrifugal blood pump with a magnetically suspended impeller," *Artif. Organs*, vol. 16, no. 3, pp. 305–308, 1992.
[7] A. Smirnov, N. Uzhegov, T. Sillanpää, J. Pyrhönen, and O. Pyrhönen, "High-speed electrical machine with active magnetic bearing system optimization," *IEEE Trans. Ind. Electron.*, vol. 64, no. 12, pp. 9876–9885, Dec. 2017.
[8] A. C. Wroblewski, J. T. Sawicki, and A. H. Pesch, "Rotor model updating and validation for an active magnetic bearing based high-speed machining spindle," *J. Eng. Gas Turbines Power*, vol. 134, no. 12, Dec. 2012.
[9] M. A. Pichot, J. P. Kajs, B. R. Murphy, A. Ouroua, B. M. Rech, R. J. Hayes, J. H. Beno, G. D. Buckner, and A. B. Palazzolo, "Active magnetic bearings for energy storage systems for combat vehicles," *IEEE Trans. Magn.*, vol. 37, no. 1, pp. 318–323, Jan. 2001.
[10] J. R. Fang, L. Z. Lin, L. G. Yan, and L. Y. Xiao, "A new flywheel energy storage system using hybrid superconducting magnetic bearings," *IEEE Trans. Appl. Supercond.*, vol. 11, no. 1, pp. 1657–1660, Mar. 2001.
[11] H. Bangcheng, Z. Shiqiang, W. Xi, and Y. Qian, "Integral design and analysis of passive magnetic bearing and active radial magnetic bearing for agile satellite application," *IEEE Trans. Magn.*, vol. 48, no. 6, pp. 1959–1966, Jun. 2012.
[12] G.-P. Ren, Z. Chen, H.-T. Zhang, Y. Wu, H. Meng, D. Wu, and H. Ding, "Design of interval type-2 fuzzy controllers for active magnetic bearing systems," *IEEE/ASME Trans. Mechatronics*, vol. 25, no. 5, pp. 2449–2459, Oct. 2020.
[13] H.-C. Chen and S.-H. Chang, "Genetic algorithms based optimization design of a PID controller for an active magnetic bearing," *Int. J. Comput. Sci. Netw. Secur.*, vol. 6, no. 12, pp. 95–99, 2006.
[14] Z. Yanhong, Z. Zhongqiao, Z. Jiansheng, and Y. Lei, "Research on PID controller in active magnetic levitation based on particle swarm optimization algorithm," *Open Autom. Control Syst. J.*, vol. 7, no. 1, pp. 1870–1874, Oct. 2015.
[15] A. Dhyani, M. K. Panda, and B. Jha, "Moth-flame optimization-based fuzzy-PID controller for optimal control of active magnetic bearing system," *Iranian J. Sci. Technol., Trans. Electr. Eng.*, vol. 42, no. 4, pp. 451–463, Dec. 2018.
[16] D. Izci, B. Hekimoğlu, and S. Ekinci, "A new artificial ecosystem-based optimization integrated with Nelder–Mead method for PID controller design of buck converter," *Alexandria Eng. J.*, vol. 61, no. 3, pp. 2030–2044, Mar. 2022, doi: 10.1016/j.aej.2021.07.037.
[17] D. Izci, S. Ekinci, and S. Mirjalili, "Optimal PID plus second-order derivative controller design for AVR system using a modified Runge Kutta optimizer and Bode's ideal reference model," *Int. J. Dyn. Control*, vol. 2022, pp. 1–18, Oct. 2022, doi: 10.1007/s40435-022-01046-9.
[18] N. Jain, G. Parmar, R. Gupta, and I. Khanam, "Performance evaluation of GWO/PID approach in control of ball hoop system with different objective functions and perturbation," *Cogent Eng.*, vol. 5, no. 1, Jan. 2018, Art. no. 1465328, doi: 10.1080/23311916.2018.1465328.
[19] D. İzci, S. Ekinci, and S. Ekinci, "Comparative performance analysis of slime mould algorithm for efficient design of proportional–integral–derivative controller," *Electrica*, vol. 21, no. 1, pp. 151–159, Jan. 2021.

[20] S. Ekinci, B. Hekimoğlu, and D. Izci, "Opposition based Henry gas solubility optimization as a novel algorithm for PID control of DC motor," *Eng. Sci. Technol., Int. J.*, vol. 24, no. 2, pp. 331–342, Apr. 2021, doi: 10.1016/j.jestch.2020.08.011.
[21] G. Lei, X. Chang, Y. Tianhang, and W. Tuerxun, "An improved mayfly optimization algorithm based on median position and its application in the optimization of PID parameters of hydro-turbine governor," *IEEE Access*, vol. 10, pp. 36335–36349, 2022, doi: 10.1109/ACCESS.2022.3160714.
[22] D. Izci, S. Ekinci, M. Kayri, and E. Eker, "A novel improved arithmetic optimization algorithm for optimal design of PID controlled and Bode's ideal transfer function based automobile cruise control system," *Evolving Syst.*, vol. 13, no. 3, pp. 453–468, Jun. 2022, doi: 10.1007/s12530-021-09402-4.
[23] S. Peicheng, L. Li, X. Ni, and A. Yang, "Intelligent vehicle path tracking control based on improved MPC and hybrid PID," *IEEE Access*, vol. 10, pp. 94133–94144, 2022, doi: 10.1109/ACCESS.2022.3203451.
[24] S. Ekinci, D. Izci, M. R. A. Nasar, R. A. Zitar, and L. Abualigah, "Logarithmic spiral search based arithmetic optimization algorithm with selective mechanism and its application to functional electrical stimulation system control," *Soft Comput.*, vol. 26, pp. 12257–12269, Apr. 2022, doi: 10.1007/s00500-022-07068-x.
[25] S. Ekinci, D. Izci, R. A. Zitar, A. R. Alsoud, and L. Abualigah, "Development of Lévy flight-based reptile search algorithm with local search ability for power systems engineering design problems," *Neural Comput. Appl.*, vol. 34, no. 22, pp. 20263–20283, Nov. 2022, doi: 10.1007/s00521-022-07575-w.
[26] I. Boussaïd, J. Lepagnot, and P. Siarry, "A survey on optimization metaheuristics," *Inf. Sci.*, vol. 237, pp. 82–117, Jul. 2013.
[27] S. Debnath and P. K. Biswas, "Design, analysis, and testing of I-type electromagnetic actuator used in single-coil active magnetic bearing," *Electr. Eng.*, vol. 103, no. 1, pp. 183–194, Feb. 2021, doi: 10.1007/s00202-020-01071-x.
[28] D. Jiang, T. Li, Z. Hu, and H. Sun, "Novel topologies of power electronics converter as active magnetic bearing drive," *IEEE Trans. Ind. Electron.*, vol. 67, no. 2, pp. 950–959, Feb. 2020.
[29] Y. He, X. He, J. Ma, and Y. Fang, "Optimization research on a switching power amplifier and a current control strategy of active magnetic bearing," *IEEE Access*, vol. 8, pp. 34833–34841, 2020, doi: 10.1109/ACCESS.2020.2974765.
[30] J. D. Lindlau and C. R. Knospe, "Feedback linearization of an active magnetic bearing with voltage control," *IEEE Trans. Control Syst. Technol.*, vol. 10, no. 1, pp. 21–31, Jan. 2002.
[31] M. Chen and C. R. Knospe, "Feedback linearization of active magnetic bearings: Current-mode implementation," *IEEE/ASME Trans. Mechatronics*, vol. 10, no. 6, pp. 632–639, Dec. 2005, doi: 10.1109/TMECH.2005.859824.
[32] S. Debnath and P. K. Biswas, "Advanced magnetic bearing device for high-speed applications with an I-type electromagnet," *Electr. Power Compon. Syst.*, vol. 48, nos. 16–17, pp. 1862–1874, 2020, doi: 10.1080/15325008.2021.1908454.
[33] J. H. Holland, *Adaptation in Natural and Artificial Systems*. Cambridge, MA, USA: MIT Press, 1975.
[34] K. Krishnakumar and D. E. Goldberg, "Control system optimization using genetic algorithms," *J. Guid., Control, Dyn.*, vol. 15, no. 3, pp. 735–740, May 1992.
[35] M. Gen, R. Cheng, and L. Lin, *Network Models and Optimization: Multiobjective Genetic Algorithm Approach*. Cham, Switzerland: Springer, 2008.
[36] R. Nambiar and P. Mars, "Adaptive IIR filtering using natural algorithms," in *Proc. IEEE Workshop Natural Algorithms Signal Process.*, vol. 740, 1993.
[37] B. Wilson and M. D. McCleod, "Low implementation cost IIR filter design using genetic algorithms," in *Proc. IEEE Workshop Natural Algorithms Signal Process.*, vol. 740, 1993.
[38] K. S. Tang, K.-F. Man, and D.-W. Gu, "Structured genetic algorithm for robust H_∞ control systems design," *IEEE Trans. Ind. Electron.*, vol. 43, no. 5, pp. 575–582, Oct. 1996.
[39] J. J. Grefenstette, "Optimization of control parameters for genetic algorithms," *IEEE Trans. Syst., Man, Cybern.*, vol. SMC-16, no. 1, pp. 122–128, Jan. 1986.
[40] Y. Davidor, "A genetic algorithm applied to robot trajectory generation," in *Handbook of Genetic Algorithms*, 1991, pp. 144–165.
[41] J. N. Amaral, K. Tumer, and J. Ghosh, "Designing genetic algorithms for the state assignment problem," *IEEE Trans. Syst., Man, Cybern.*, vol. 25, no. 4, pp. 687–694, Apr. 1995.
[42] L. Yao and W. A. Sethares, "Nonlinear parameter estimation via the genetic algorithm," *IEEE Trans. Signal Process.*, vol. 42, no. 4, pp. 927–935, Apr. 1994.
[43] Y.-S. Yen, Y.-K. Chan, H.-C. Chao, and J. H. Park, "A genetic algorithm for energy-efficient based multicast routing on MANETs," *Comput. Commun.*, vol. 31, no. 10, pp. 2632–2641, Jun. 2008.
[44] T. Blickle and L. Thiele, "A comparison of selection schemes used in evolutionary algorithms," *Evol. Comput.*, vol. 4, no. 4, pp. 361–394, Dec. 1996.
[45] T. Bäck and H.-P. Schwefel, "An overview of evolutionary algorithms for parameter optimization," *Evol. Comput.*, vol. 1, pp. 1–23, Dec. 1993.
[46] D. E. Goldberg, *Genetic Algorithms in Search, Optimization, and Machine Learning*. Boston, MA, USA: Addison Reading, 1989.
[47] J. Kennedy and R. Eberhart, "Particle swarm optimization," in *Proc. Int. Conf. Neural Netw.*, vol. 4, 1995, pp. 1942–1948.
[48] X.-S. Yang, *Nature-Inspired Optimization Algorithms*. New York, NY, USA: Academic, 2020.
[49] Y. Zhang, S. Wang, and G. Ji, "A comprehensive survey on particle swarm optimization algorithm and its applications," *Math. Probl. Eng.*, vol. 2015, Jan. 2015, Art. no. 931256, doi: 10.1155/2015/931256.
[50] J. Yang, L. He, and S. Fu, "An improved PSO-based charging strategy of electric vehicles in electrical distribution grid," *Appl. Energy*, vol. 128, no. 3, pp. 82–92, Sep. 2014.
[51] S. K. Pandey, S. R. Mohanty, N. Kishor, and J. P. S. Catalão, "Frequency regulation in hybrid power systems using particle swarm optimization and linear matrix inequalities based robust controller design," *Int. J. Elect. Power Energy Syst.*, vol. 63, pp. 887–900, Dec. 2014.
[52] X. Guo, C. Wang, and R. Yan, "An electromagnetic localization method for medical micro-devices based on adaptive particle swarm optimization with neighborhood search," *Measurement*, vol. 44, no. 5, pp. 852–858, Jun. 2011.
[53] M. Karabulut and T. Ibrikci, "A Bayesian scoring scheme based particle swarm optimization algorithm to identify transcription factor binding sites," *Appl. Soft Comput.*, vol. 12, no. 9, pp. 2846–2855, Sep. 2012.
[54] W. Zhang, H. Xie, B. Cao, and A. M. K. Cheng, "Energy-aware real-time task scheduling for heterogeneous multiprocessors with particle swarm optimization algorithm," *Math. Problems Eng.*, vol. 2014, pp. 1–9, Jan. 2014.
[55] X.-S. Yang and S. Deb, "Cuckoo search via Lévy flights," in *Proc. World Congr. Nature Biologically Inspired Comput. (NaBIC)*, 2009, pp. 210–214.
[56] D. Chitara, K. R. Niazi, A. Swarnkar, and N. Gupta, "Cuckoo search optimization algorithm for designing of a multimachine power system stabilizer," *IEEE Trans. Ind. Appl.*, vol. 54, no. 4, pp. 3056–3065, Jul./Aug. 2018.
[57] J. I. Ababneh and M. M. Khodier, "Design and optimization of enhanced magnitude and phase response IIR full-band digital differentiator and integrator using the cuckoo search algorithm," *IEEE Access*, vol. 10, pp. 28938–28948, 2022.
[58] H. H. Issa and S. M. E. Ahmed, "FPGA implementation of floating point based cuckoo search algorithm," *IEEE Access*, vol. 7, pp. 134434–134447, 2019.
[59] X.-S. Yang and S. Deb, "Cuckoo search: Recent advances and applications," *Neural Comput. Appl.*, vol. 24, no. 1, pp. 169–174, Jan. 2014.
[60] I. Fister, X.-S. Yang, and D. Fister, "Cuckoo search: A brief literature review," *Cuckoo Search and Firefly Algorithm*, 2014, pp. 49–62.

SURAJ GUPTA (Graduate Student Member, IEEE) received the B.Tech. degree from Uttar Pradesh Technical University, India, in 2013, and the M.Tech. degree in power electronics and drives from the National Institute of Technology Mizoram, Aizawl, India, in 2018, where he is currently pursuing the Ph.D. degree with the Department of Electrical and Electronics Engineering.

PABITRA KUMAR BISWAS (Member, IEEE) received the B.Tech. degree from the Asansol Engineering College, WBUT, India, the M.E. degree in power electronics and drives from Bengal Engineering and Science University, West Bengal, India, in 2007, and the Ph.D. degree in electrical engineering from the National Institute of Technology, Durgapur, India, in 2013. He was the HoD of the EEE Department, from February 2015 to August 2019. He is currently working as an Associate Professor in electrical and electronics engineering with the National Institute of Technology Mizoram, India. He has about 14 years of academic as well as research experience. He has guided five Ph.D. students and more than ten M.Tech. students and ten more are pursuing their research at present. He has reviewed papers in reputed international conference and journals. He has successfully organized a GIAN course, a two short term course, and a FDP (ATAL). He has completed one DST-SERB Project. He has published a number of research papers in national/international conference and records/journals. He has a book and more than six book chapters and filed three patents. His research interests include electromagnetic levitation systems, active magnetic bearing, power electronics converters, PMSM and BLDC motor drives, electric vehicles, and renewable energy. He is a member of the Institute of Engineers and the International Association of Engineers. He is also a fellow of the SAS Society (FSASS). He has received the Best Paper Award and the Best Researcher Award (International Scientist Awards on Engineering, Science and Medicine).

SUKANTA DEBNATH was born in Tripura, India, in 1986. He received the B.Tech. degree from WBUT, India, the M.Tech. degree from NIT Agartala, Tripura, and the Ph.D. degree in electrical engineering from NIT Mizoram, Aizawl, India. He is currently working as an Assistant Professor in electrical and electronics engineering with NIT Mizoram.

ANUMOY GHOSH is currently working as an Assistant Professor with the Department of Electronics and Communication Engineering, National Institute of Technology Mizoram. His research interests include antennas, electromagnetic periodic structures, RF energy scavenging, and microwave passive circuits.

THANIKANTI SUDHAKAR BABU (Senior Member, IEEE) received the B.Tech. degree from Jawaharlal Nehru Technological University, Ananthapur, India, in 2009, the M.Tech. degree in power electronics and industrial drives from Anna University, Chennai, India, in 2011, and the Ph.D. degree from VIT University, Vellore, India, in 2017.

He has completed the Postdoctoral Fellowship from the Department of Electrical Power Engineering, Institute of Power Engineering, University Tenaga Nasional (UNITEN), Malaysia. He is currently working as an Associate Professor with the Department of Electrical and Electronics Engineering, Chaitanya Bharathi Institute of Technology, Hyderabad. He has published more than 140 research articles in various renowned international journals. His research interests include design and implementation of solar PV systems, renewable energy resources, power management for hybrid energy systems, storage systems, fuel cell technologies, electric vehicle, and smart grid. He has been acting as an Editorial Board Member and a Reviewer for various reputed journals, such as the IEEE and IEEE Access, IET, Elsevier, and Taylor & Francis.

HOSSAM M. ZAWBAA received the B.Sc. and M.Sc. degrees from the Faculty of Computers and Information, Cairo University, Giza, Egypt, in 2008 and 2012, respectively, and the Ph.D. degree from Babeş-Bolyai University, Cluj-Napoca, Romania, in 2018. He is currently an Assistant Professor with the Faculty of Computers and Artificial Intelligence, Beni-Suef University, Beni Suef, Egypt. He has over 100 research publications in peer-reviewed reputed journals and international conference proceedings. His research interests include computational intelligence, machine learning, computer vision, and natural language understanding. He has been awarded the State Encouragement Award for the year 2020 in engineering sciences from the Academy of Scientific Research and Technology, Egypt. He was rated as one of the top 2% scientists worldwide by Stanford in AI, in 2020, 2021, and 2022.

SALAH KAMEL received the international Ph.D. degree from the University of Jaén, Spain (Main), and Aalborg University, Denmark (Host), in January 2014. He is currently an Associate Professor with the Department of Electrical Engineering, Aswan University. He is also a Leader of the Advanced Power Systems Research Laboratory (APSR Laboratory), Power Systems Research Group, Aswan, Egypt. His research interests include power system analysis and optimization, smart grid, and renewable energy systems.